

Co-doped $BaFe_2As_2$ Josephson junction fabricated with a focused helium ion beam

Ziwen Chen(陈紫雯), Yan Zhang(张焱), Ping Ma(马平), Zhongtang Xu(徐中堂), Yulong Li(李宇龙), Yue Wang(王越), Jianming Lu(路建明), Yanwei Ma(马衍伟), and Zizhao Gan(甘子钊)

Citation: Chin. Phys. B, 2024, 33 (**4**): 047405. DOI: 10.1088/1674-1056/ad21f7
Journal homepage: http://cpb.iphy.ac.cn; http://iopscience.iop.org/cpb

What follows is a list of articles you may be interested in

Anomalous spin Josephson effect in spin superconductors

Wen Zeng(曾文) and Rui Shen(沈瑞)
Chin. Phys. B, 2024, 33 (**3**): 037401. DOI: 10.1088/1674-1056/ad1982

Josephson vortices and intrinsic Josephson junctions in the layered iron-based superconductor $Ca_{10}(Pt_3As_8)((Fe_{0.9}Pt_{0.1})_2As_2)_5$

Qiang-Tao Sui(随强涛) and Xiang-Gang Qui(邱祥冈)
Chin. Phys. B, 2022, 31 (**9**): 097403. DOI: 10.1088/1674-1056/ac76ae

Asymmetric Fraunhofer pattern in Josephson junctions from heterodimensional superlattice V_5S_8

Juewen Fan(范珏雯), Bingyan Jiang(江丙炎), Jiaji Zhao(赵嘉佶), Ran Bi(毕然), Jiadong Zhou(周家东), Zheng Liu(刘政), Guang Yang(杨光), Jie Shen(沈洁), Fanming Qu(屈凡明), Li Lu(吕力), Ning Kang(康宁), and Xiaosong Wu(吴孝松)
Chin. Phys. B, 2022, 31 (**5**): 057402. DOI: 10.1088/1674-1056/ac5d30

Ac Josephson effect in Corbino-geometry Josephson junctions constructed on Bi_2Te_3 surface

Yunxiao Zhang(张云潇), Zhaozheng Lyu(吕昭征), Xiang Wang(王翔), Enna Zhuo(卓恩娜), Xiaopei Sun(孙晓培), Bing Li(李冰), Jie Shen(沈洁), Guangtong Liu(刘广同), Fanming Qu(屈凡明), and Li Lü(吕力)
Chin. Phys. B, 2022, 31 (**10**): 107402. DOI: 10.1088/1674-1056/ac89d4

Josephson current in an irradiated Weyl semimetal junction

Han Wang(王含) and Rui Shen(沈瑞)
Chin. Phys. B, 2021, 30 (**7**): 077406. DOI: 10.1088/1674-1056/ac0348

RAPID COMMUNICATION

Co-doped $BaFe_2As_2$ Josephson junction fabricated with a focused helium ion beam

Ziwen Chen(陈紫雯)[1,2,3,4], Yan Zhang(张焱)[1,2,3,4,†], Ping Ma(马平)[1,2,3,4,‡], Zhongtang Xu(徐中堂)[5,§], Yulong Li(李宇龙)[1,2,3,4], Yue Wang(王越)[1,2,3,4], Jianming Lu(路建明)[1,2,3,4], Yanwei Ma(马衍伟)[5], and Zizhao Gan(甘子钊)[1,2,3,4]

[1] *Applied Superconductivity Research Center, Peking University, Beijing* 100871, *China*
[2] *State Key Laboratory for Artificial Microstructure and Mesoscopic Physics, Peking University, Beijing* 100871, *China*
[3] *Institute of Condensed Matter Physics, School of Physics, Peking University, Beijing* 100871, *China*
[4] *Yangtze Delta Institute of Optoelectronics, Peking University, Beijing* 100871, *China*
[5] *Key Laboratory of Applied Superconductivity, Institute of Electrical Engineering, Chinese Academy of Sciences, Beijing* 100190, *China*

(Received 29 December 2023; revised manuscript received 14 January 2024; accepted manuscript online 24 January 2024)

Josephson junction plays a key role not only in studying the basic physics of unconventional iron-based superconductors but also in realizing practical application of thin-film based devices, therefore the preparation of high-quality iron pnictide Josephson junctions is of great importance. In this work, we have successfully fabricated Josephson junctions from Co-doped $BaFe_2As_2$ thin films using a direct junction fabrication technique which utilizes high energy focused helium ion beam (FHIB). The electrical transport properties were investigated for junctions fabricated with various He^+ irradiation doses. The junctions show sharp superconducting transition around 24 K with a narrow transition width of 2.5 K, and a dose correlated foot-structure resistance which corresponds to the effective tuning of junction properties by He^+ irradiation. Significant J_c suppression by more than two orders of magnitude can be achieved by increasing the He^+ irradiation dose, which is advantageous for the realization of low noise ion pnictide thin film devices. Clear Shapiro steps are observed under 10 GHz microwave irradiation. The above results demonstrate the successful fabrication of high quality and controllable Co-doped $BaFe_2As_2$ Josephson junction with high reproducibility using the FHIB technique, laying the foundation for future investigating the mechanism of iron-based superconductors, and also the further implementation in various superconducting electronic devices.

Keywords: focused helium ion beam, Co doped $BaFe_2As_2$, Josephson junction

PACS: 74.70.Xa, 85.25.Cp, 07.78.+s, 03.75.Lm **DOI:** 10.1088/1674-1056/ad21f7

1. Introduction

The discovery of iron-based superconductors[1–6] has spurred extensive investigations not only in unveiling the underlying mechanism for their unconventional superconductivity,[7–14] but also in superconducting applications. It is suggested by these researches that the iron pnictides are novel high temperature superconductors with multi-bands electrical structure, which typically have a weak anisotropic band structure on the Fermi surface.[15–18] The intrinsic electrical structure gives iron pnictides remarkable properties, e.g., high upper critical magnetic field, high critical current density which is insensitive to grain boundaries, and also robustness to doping impurity, which make them favorable for making superconducting wires and tapes for electrical applications.[19,20]

When it comes to the field of superconducting electronics based on Josephson junctions (JJs), however, the short coherence length and the insensitive nature of iron-based superconductor to grain boundaries makes it difficult to fabricate JJs, which is disadvantageous not only for the exploration of the basic physics of the iron-based superconductors but also for the development of iron pnictides based superconducting electronic devices such as superconducting quantum interference devices (SQUIDs)[21] and terahertz (THz) mixers.[22] Among the iron pnictides, Co doped $BaFe_2As_2$ (Ba122:Co) thin film prepared by pulsed laser deposition (PLD) has improved crystallinity and superconducting properties, which is suitable for fabricating high quality junctions and thin-film based devices. Hybrid junction technique[23] and bi-crystal junction technique[21,24] are two main techniques currently used for fabricating pnictide Josephson junctions. For hybrid junctions, the complexity of fabrication process has made it hard to control the junction parameters flexibly. For bi-crystal junctions, the s-wave-like paring symmetry nature of Ba122:Co with weak anisotropy makes it difficult to suppress the critical current density J_c[20,25,26] for the purpose of achieving weak links even at large grain boundary angles, while the cuprate materials with strong anisotropy, e.g, YBCO, could show a more

†Corresponding author. E-mail: zhang_yan@pku.edu.cn
‡Corresponding author. E-mail: maping@pku.edu.cn
§Corresponding author. E-mail: ztxu@mail.iee.ac.cn

© 2024 Chinese Physical Society and IOP Publishing Ltd

significantly J_c suppression.[27] This means that for Ba122:Co bi-crystal junctions, a low critical current I_c could be difficult to achieve, while a small I_c value is generally more favorable for thin film devices such as low noise SQUIDs. Therefore, it is necessary to figure out a both controllable and flexible way to fabricate high quality Josephson junctions with wide range of junction parameters for the purpose of better understanding the superconductivity of iron pnictides and for potential device applications.

With the development of helium ion microscope (HIM), the focused helium ion beam (FHIB) currently emerges as a new junction technique and is proven to be efficient in fabricating Josephson junctions from many unconventional superconducting materials, such as $YBa_2Cu_3O_{7-\delta}$,[28] MgB_2,[29] and $Bi_2Sr_2CaCuO_{8+x}$.[30] Rather than bi-crystal junctions which rely on the anisotropy properties of the superconductor and naturally formed defects within the misaligned grain boundary, FHIB technique could suppress the superconductivity by directly inducing artificial defects and dopant vacancies within the irradiation region with a 30 keV He^+ beam irradiation to effectively create the weak links, and the junction parameters are easily controlled with appropriate ion doses. Besides, ideally it could provide a focused He^+ beam with a beam size of around 0.5 nm, and the beam flux could remain stable during a long period of time with slight deviations. Since the coherence length of Ba122:Co is about 2.5 nm[31] and the FHIB can create a narrow junction region, it could be a feasible method to direct write Ba122 Josephson junctions with very high reproducibility.

While there has been study investigating the effect of 30 keV FHIB irradiation on the superconducting properties of Ba122:Co film,[32] however, to the best of our knowledge the fabrication of FHIB Ba122:Co Josephson junction using this technique has not yet been reported so far, and the properties of FHIB Ba122:Co junctions remain unclear. In this work, we report the first successful fabrication of Josephson junctions from superconducting material of Ba122:Co using a 30 keV FHIB and the junction properties are investigated. Superconducting transition and electric transport properties of Ba122:Co junctions irradiated with various of He^+ doses are presented. The junction critical current density is determined from the current–voltage (I–V) characteristics and compared to illustrate the effective tuning of the junction properties with the variation of He^+ dose. Clear Shapiro steps are also observed under 10 GHz microwave radiation. Our work shows the high quality and controllability of Ba122:Co Josephson junctions fabricated using the FHIB technique, which could be helpful for the future development of superconducting electronics and related applications based on iron pnictide materials.

2. Experimental details

The fabrication process of the Co doped $BaFe_2As_2$ (Ba122:Co) FHIB junction is shown in Fig. 1. The Ba122:Co thin films were grown by pulsed laser deposition (PLD) utilizing a KrF excimer laser with the wavelength of 248 nm on CaF_2 single crystal substrates (5×5 mm^2), which had been demonstrated to have superior superconducting properties compared with films deposited on other substrates.[33] The targets of nominal composition $BaFe_{1.84}Co_{0.16}As_2Y_2O_3$ ablated in PLD were synthesized by the solid-state reaction method. The optimal fabrication conditions to obtain high-quality epitaxial thin films were a 1.4 J·cm^{-2} laser energy density with a repetition rate of 9 Hz, a 55 mm distance between the target and the substrate, and a substrate temperature

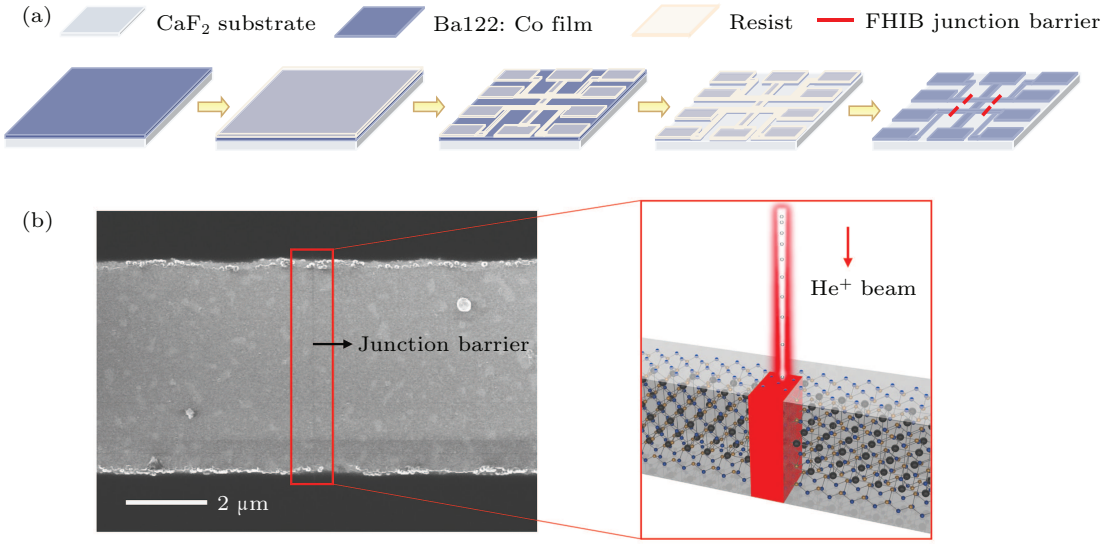


Fig. 1. (a) Schematic diagrams depicting the fabrication process of FHIB Ba122:Co Josephson junction. The red lines indicate the location of junction barrier introduced by He^+ irradiation. (b) Left panel shows HIM image of the junction region for FHIB junction irradiated with dose of $D = 300$ ions/nm. The black arrow indicates the junction barrier after the irradiation process. Right panel is a schematic representation of an FHIB creating Josephson junction barrier on a Ba122:Co bridge.

of 825 °C in a base pressure better than 10^{-7} Torr. The films were successively cooled down to room temperature at a rate of 10 °C·min^{-1}. The thickness of the as-prepared thin films (about 50 nm) was measured by a KLA AlphaStep D600 step profiler. Such a thickness could prevent significant scattering of the incident He^+ beam into Ba122:Co thin films to ensure a uniform junction barrier. After the preparation of Ba122 film, a standard UV lithography and an Ar ion milling process were performed to define the electrical pads and the microbridges for further junction writing process. The width of the microbridge is about 5 μm. Then we loaded the sample into the high vacuum chamber of Zeiss Orion HIM at room temperature. The FHIB Josephson junctions were written on the bridges with a line-scan mode with a beam current of about 1 pA. The defined line consisted of a series of pixels and the dwell time of the He^+ beam at each of these pixels was set at 1 μs. Several repeats were performed during the irradiation process to attain the desired dose value. A spacing of 0.25 nm between pixels was chosen to ensure sufficient overlap of the He^+ beam. We irradiated different bridges prepared on the same film with He^+ doses ranging from 100 ions/nm to 300 ions/nm. The samples were then packaged onto a sample holder. The electrical transport measurements were carried out on samples with a standard four-probe method in a physical properties measurement system (PPMS, Quantum Design). The microwave radiation was introduced via an antenna placed above the sample connecting a microwave source at frequency of 10 GHz through a coaxial cable. A self-written program was used to control the PPMS and perform the measurements.

3. Results and discussion

In order to obtain information regarding influences of the He^+ irradiation dose on Ba122:Co Josephson junctions, resistance versus temperature (R–T) characteristics measurements were performed for all junctions with various He^+ doses. Figure 2(a) shows the R–T curves normalized by resistance at 300 K of junctions with dose $D = 0$, 100, 150, 200, 300 ions/nm. Figure 2(b) shows zoom-in view of the superconducting transition region. Junctions with different irradiation doses in the figure all show similar superconducting transition started from $T_c^{onset} = 24.3$ K with a narrow transition width of about 2.5 K. The foot-structure-like resistance for junctions with He^+ irradiation shown on the inset of Fig. 2(b), which arises from the thermally activated phase slippage when the Josephson coupling energy is comparable to or smaller than the thermal fluctuation, has also been observed in our previous study on FHIB Josephson junctions fabricated from cuprate material $YBa_2Cu_3O_{7-\delta}$.[34] With a higher irradiation dose, the foot-structure-like resistance is broader, and the height of this structure also becomes larger. Such a variation of the foot-structure resistance indicates the effective tuning of Josephson coupling energy (or I_c) by He^+ irradiation.

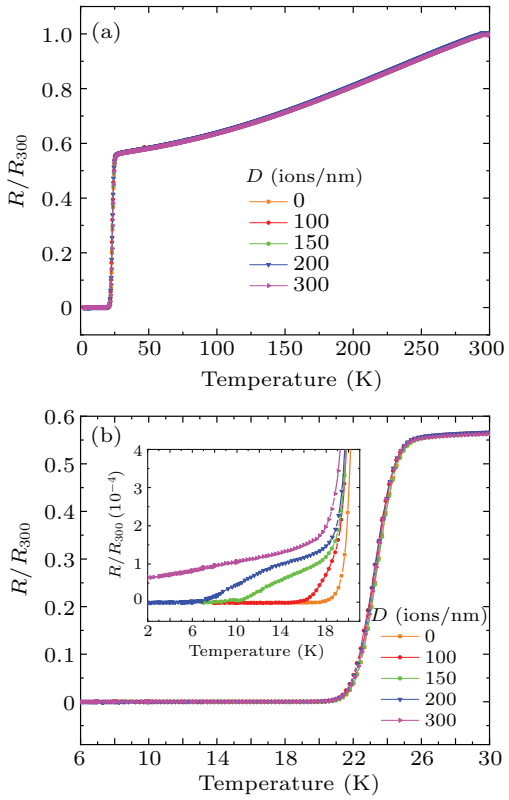


Fig. 2. (a) The R–T characteristic of FHIB junctions with He^+ dose ranging from 0 ions/nm (without He^+ irradiation) to 300 ions/nm. (b) Zoom-in view of (a) showing the superconducting transition region. The inset illustrates the variation of the foot-structure-like resistance of Ba122:Co junctions with varying the He^+ dose.

Figures 3(a) and 3(b) respectively show the I–V curves of junctions with He^+ irradiation dose D of 200 ions/nm and 300 ions/nm measured at several temperatures. The figures clearly show that larger dose D results in a smaller junction I_c, which is in line with the increase of the foot-structure resistance with larger D as shown in Fig. 2(b). Figure 3(c) presents the temperature dependence of I_cR_n product for junctions shown in Figs. 3(a) and 3(b), showing a nearly linear behavior of I_cR_n decrease with increasing temperature. We note that for junctions with $D = 200$ ions/nm, the I_cR_n value and its temperature dependence are close to those of Ba122:Co bicrystal junctions with grain boundary misorientation angle of 30°.[21] Besides temperature dependence, it can also be clearly seen from the figure that the 300 ions/nm junction with smaller J_c value exhibits smaller I_cR_n, which was found to be a typical behavior of grain boundary junctions featuring defects within the grain boundaries. These results may validate that the weak link behavior of FHIB Ba122:Co junctions arises from the defect concentrations within the junction barrier.

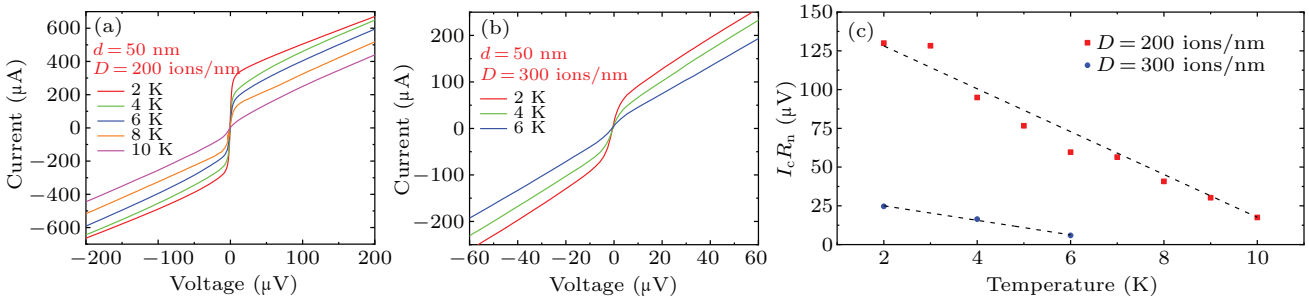


Fig. 3. The *I*–*V* curves measured at different temperatures for junctions with irradiation dose (a) $D = 200$ ions/nm and (b) $D = 300$ ions/nm, respectively. (c) Temperature dependence of I_cR_n for junctions with $D = 200$ ions/nm, 300 ions/nm. The black dashed lines are used to guide the eyes.

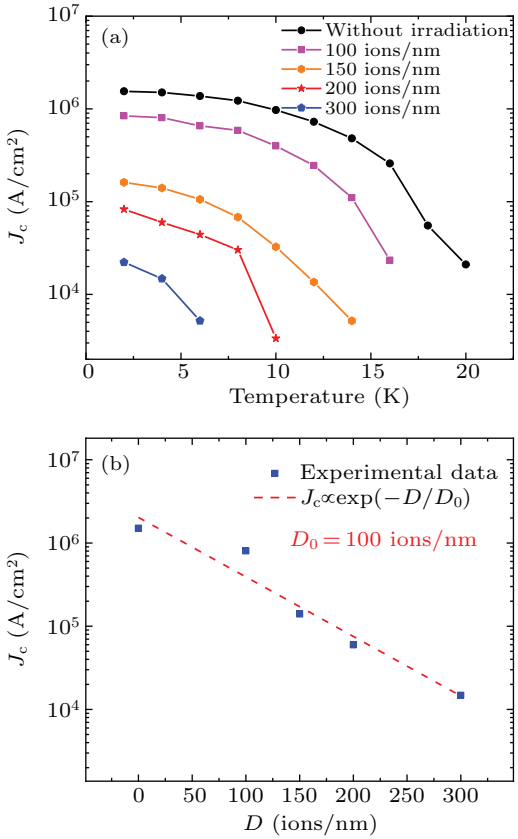


Fig. 4. (a) The J_c versus T for FHIB junctions with various He^+ doses. (b) J_c versus He^+ irradiation dose measured at 4 K.

Figure 4(a) shows the temperature dependence of critical current density J_c as extracted from the measured current–voltage (*I*–*V*) curves for junctions with different He^+ irradiation dose D. As can be seen from the figure, J_c is suppressed by about 2 orders of magnitude when increasing the He^+ irradiation dose from 0 to 300 ions/nm. Such a considerable decrease of J_c of Ba122:Co FHIB junctions demonstrates the formation of effective weak links which might arise from the rapid increase of defect concentrations induced by He^+ irradiation, and the relation between J_c and D shows the flexible modulation ability of He^+ beam on junction J_c. We note that the temperature dependence of J_c and the specific J_c value for our FHIB junction with dose of 150 ions/nm are almost the same as those of 30° misorientation Ba122:Co bi-crystal junction,[24] which only suppresses the J_c by about one order of magnitude compared with that of Ba122:Co thin films. For bi-crystal Ba122:Co junctions, the further suppression of J_c could be hard even with larger misorientation angles.[26] The J_c value at 4 K for FHIB junction is plotted in Fig. 4(b) as a function of D. A decreasing trend of junction J_c with increasing D can be clearly seen on the figure, which can be fitted by an empirical formula $J_c \propto \exp(-D/D_0)$ with $D = 100$ ions/nm.[35] We note that a similar trend has also been observed for FHIB junctions made from YBCO thin films with similar D value.[34] This suggests that the exponential behavior of J_c with respect to dose D could be universal for FHIB junctions fabricated from different superconducting materials, which is not subjected to the material electronic properties since YBCO has significantly different electronic properties with Ba122:Co. From the exponential J_c suppression with respect to the increase of D as shown in Fig. 4(b), we find that J_c suppression of 2 or even larger orders of magnitude which corresponds to I_c at the level of several tens of μA could easily be achieved by applying a larger irradiation dose with our current junction geometry, which should be sufficient for the realization of low noise devices based on Ba122:Co, e.g., SQUIDs. Therefore, Ba122:Co junction based on FHIB technique has promising prospect for future device applications.

We have also investigated the AC characteristics of our FHIB Ba122:Co junctions under microwave radiation at a frequency of $f = 10$ GHz to further verify the high quality of our FHIB Ba122:Co junctions. Figures 5(a) and 5(b) respectively show the *I*–*V* curves measured with a 10 GHz microwave radiation for junctions with dose D of 200 ions/nm and 300 ions/nm. The *I*–*V* curves without microwave radiation are also presented here to show the suppression of junction I_c. As can be seen in Fig. 5(a), the presented *I*–*V* curves feature clear Shapiro steps. It is well known from the theory that the Shapiro steps appear at the specific voltage of $V = nhf/(2e)$, where n is an integer number, f represents the microwave frequency, and $h/(2e)$ is the flux quantum. From the experimental results shown in Fig. 5(a) we find that the steps appear about every 20 μV at the *I*–*V* curves, which comply well with the theoretical one as calculated from the above formula. We also note that in Fig. 5(a), the height of the steps varies as well by varying the microwave power. With increasing power, the height of the first Shapiro step increases first and reaches a

maximum at 14 dBm within the power range of our measurements, then it decreases progressively to zero over the range of 15 dBm to 17 dBm. As shown in Fig. 5(b), for junctions with $D = 300$ ions/nm, when in the absence of microwave irradiation, the small junction I_c results in a small Josephson coupling that is comparable with thermal fluctuation. Therefore, an obvious slope can also be observed in the I–V curve due to the phase slippage for the junction with $D = 300$ ions/nm, which is hard for the junction to exhibit apparent steps. One can also find that while the junction I_c is completely suppressed when the microwave power is set at 13 dBm, the first step at about 20 μV can still be observed as indicated by the black arrow. Figure 5 shows that junctions with dose of 200 ions/nm can exhibit pronounced AC Josephson effect compared with junction irradiated with higher dose of up to 300 ions/nm.

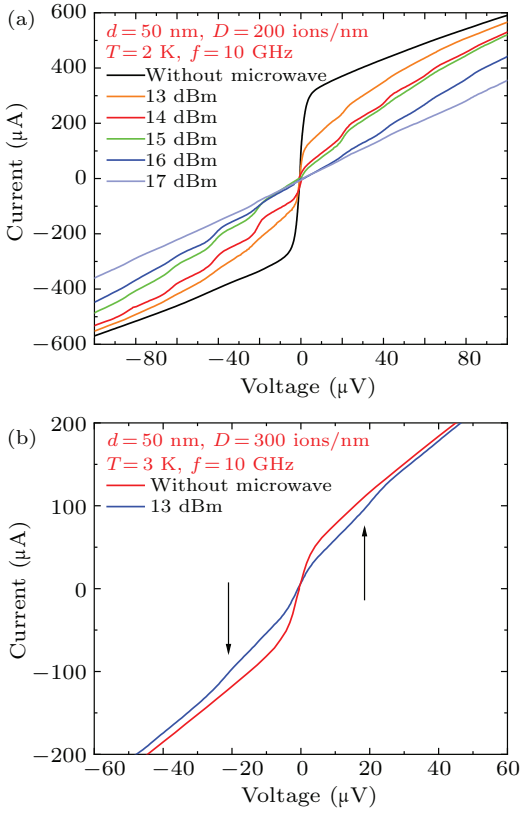


Fig. 5. The I–V curves exhibiting Shapiro steps measured under different microwave radiation power for junctions (a) with dose $D = 200$ ions/nm measured at 2 K and (b) $D = 300$ ions/nm measured at 3 K. The I–V curves without microwave radiation are also presented to show the significant I_c suppression in the presence of microwave radiation.

Besides the high junction quality, high junction parameter consistency has also been found in our FHIB Ba122:Co junctions. Figure 6 presents two I–V curves and the corresponding differential resistance $\mathrm{d}V/\mathrm{d}I$ of two FHIB junctions fabricated on the same chip with the same He^+ dose of 200 ions/nm. The critical currents I_c as shown in Fig. 6(a) for the two junctions are almost identical, while the two I–V curves at bias current exceeding I_c are slightly deviated. This can be seen more clearly in Fig. 6(b). The deviation of normal resistance R_n of the two junctions, which could be represented by the differential resistance $\mathrm{d}V/\mathrm{d}I$ at large bias current, e.g., larger than 600 μA, is determined to be less than 10%. The deviation of two junctions at bias current larger than I_c and the asymmetric behavior may be caused by the inhomogeneous junction interface which needs to be further improved. Nonetheless, such a low deviation of junction parameters for junctions using FHIB technique is superior to the commonly used bi-crystal junction technique whose parameter deviation could be larger than 20%, as had been reported in other material systems such as YBCO.[36] As a comparison, we have demonstrated the high consistency of YBCO FHIB junctions using this FHIB technique with junction parameter deviation less than 10%.[34]

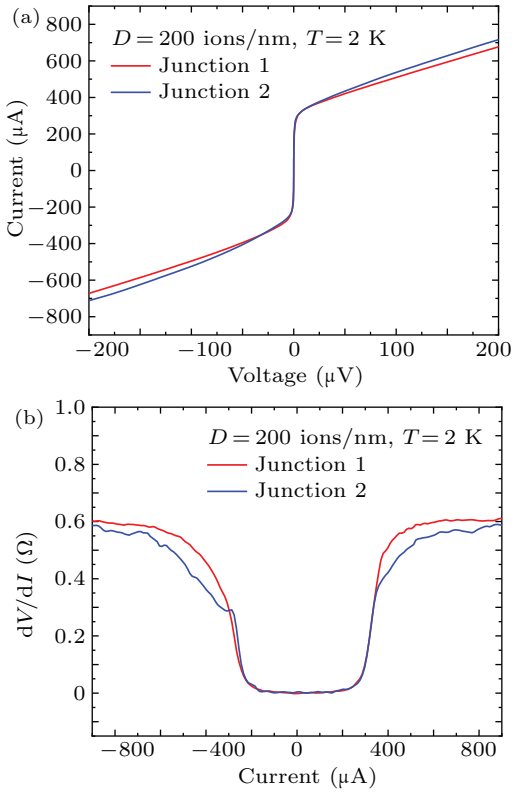


Fig. 6. (a) The I–V curves of two junctions on the same Ba122:Co film at 2 K. (b) Differential resistance $\mathrm{d}V/\mathrm{d}I$ (Ω) versus current of two junctions on a same Ba122:Co film at 2 K.

The above results clearly demonstrate the high quality, larger parameter range with high tunability, as well as high fabrication reliability of Ba122:Co junctions fabricated with the FHIB technique which could serve as a promising tool for further researches on the superconducting mechanism and future implementation of various superconducting electronic devices based on iron pnictide materials.

4. Conclusion and perspectives

We have successfully fabricated high quality and controllable Co-doped $BaFe_2As_2$ Josephson junction using the focused helium ion beam (FHIB) technique with a dose range

of 100–300 ions/nm. The *R*–*T* curves of the fabricated junctions with different irradiation doses demonstrate effectively tuning of the junction barrier after He^+ irradiation. The *I*–*V* curves measured at different temperatures for our FHIB junctions show significant suppression of the junction critical current density under He^+ irradiation compared with a bare Ba122 bridge, which show that the FHIB junction technique is more favorable than the typically bi-crystal junction technique in fabricating low noise thin film devices such as SQUIDs. AC Josephson effect of the junctions was also investigated, showing apparent Shapiro steps for a junction with dose of 200 ions/nm while varying the microwave radiation power. Our work demonstrates the advantages on both junction quality and parameter tunability, and also the high fabrication reliability of Co-doped $BaFe_2As_2$ Josephson junctions using FHIB technique, which lays the foundation for further investigating the mechanism of iron-based superconductors, and may also be benefit to the advancement of various scalable superconducting electronic thin film devices based on iron-based superconductors.

Acknowledgements

Project supported by the National Key Research and Development Program of China (Grant Nos. 2020YFF01014706 and 2017YFC0601901) and the National Natural Science Foundation of China (Grant Nos. 61571019 and 52177026). The authors would like to acknowledge the valuable contributions of Lifeng Tian, Technical Institute of Physics and Chemistry, Chinese Academy of Sciences, for his help in use of helium ion microscope; and Ziqing Chen for the artistic drawing of the Ba122:Co junction fabricated by a focused helium ion beam.

References

[1] Kamihara Y, Watanabe T, Hirano M and Hosono H 2008 *J. Am. Chem. Soc.* **130** 3296
[2] Rotter M, Tegel M and Johrendt D 2008 *Phys. Rev. Lett.* **101** 107006
[3] Wang X C, Liu Q Q, Lv Y X, Gao W B, Yang L X, Yu R C, Li F Y and Jin C Q 2008 *Solid State Commun.* **148** 538
[4] Hsu F C, Luo J Y, Yeh K W, Chen T K, Huang T W, Wu P M, Lee Y C, Huang Y L, Chu Y Y, Yan D C and Wu M K 2008 *Proc. Natl. Acad. Sci. USA* **105** 14262
[5] Sefat A S, Jin R, McGuire M A, Sales B C, Singh D J and Mandrus D 2008 *Phys. Rev. Lett.* **101** 117004
[6] Ren Z A, Lu W, Yang J, Yi W, Shen X L, Li Z C, Che G C, Dong X L, Sun L L, Zhou F and Zhao Z X 2008 *Chin. Phys. Lett.* **25** 2215
[7] Scalapino D J 2012 *Rev. Mod. Phys.* **84** 1383
[8] Fernandes R M, Chubukov A V and Schmalian J 2014 *Nat. Phys.* **10** 97
[9] Zhao J, Huang Q, de la Cruz C, Li S L, Lynn J W, Chen Y, Green M A, Chen G F, Li G, Li Z, Luo J L, Wang N L and Dai P C 2008 *Nat. Mater.* **7** 953
[10] Dong X L, Jin K, Yuan D N, Zhou H X, Yuan J, Huang Y L, Hua W, Sun J L, Zheng P, Hu W, Mao Y Y, Ma M W, Zhang G M, Zhou F and Zhao Z X 2015 *Phys. Rev. B* **92** 064515
[11] Mu G, Zeng B, Cheng P, Wang Z S, Fang L, Shen B, Shan L, Ren C and Wen H H 2010 *Chin. Phys. Lett.* **27** 037402
[12] Wang D, Lu H Y and Wang Q H 2013 *Chin. Phys. Lett.* **30** 077404
[13] Chen G F, Li Z, Li G, Hu W Z, Dong J, Zhou J, Zhang X D, Zheng P, Wang N L and Luo J L 2008 *Chin. Phys. Lett.* **25** 3403
[14] Zhao L, Liu H Y, Zhang W T, Meng J Q, Jia X W, Liu G D, Dong X L, Chen G F, Luo J L, Wang N L, Lu W, Wang G L, Zhou Y, Zhu Y, Wang X Y, Xu Z Y, Chen C T and Zhou X J 2008 *Chin. Phys. Lett.* **25** 4402
[15] Mazin, II, Singh D J, Johannes M D and Du M H 2008 *Phys. Rev. Lett.* **101** 057003
[16] Nakamura H, Machida M, Koyama T and Hamada N 2009 *J. Phys. Soc. Jpn.* **78** 123712
[17] Mazin, II and Schmalian J 2009 *Phys. C* **469** 614
[18] Johnston D C 2010 *Advances in Physics* **59** 803
[19] Huang Y L, Feng Z P, Ni S L, Li J, Hu W, Liu S B, Mao Y Y, Zhou H X, Zhou F, Jin K, Wang H B, Yuan J, Dong X L and Zhao Z X 2017 *Chin. Phys. Lett.* **34** 077404
[20] Ma Y W 2012 *Superconductor Science & Technology* **25** 113001
[21] Katase T, Ishimaru Y, Tsukamoto A, Hiramatsu H, Kamiya T, Tanabe K and Hosono H 2010 *Supercond. Sci. Technol.* **23** 082001
[22] Wang T, Yu A, Li C, Liu Y, Peng W, Jiang D and Mu G 2023 *Scientia Sinica: Physica, Mechanica et Astronomica* **53** 127414
[23] Zhang X H, Oh Y S, Liu Y, Yan L Q, Kim K H, Greene R L and Takeuchi I 2009 *Phys. Rev. Lett.* **102** 147002
[24] Katase T, Ishimaru Y, Tsukamoto A, Hiramatsu H, Kamiya T, Tanabe K and Hosono H 2010 *Appl. Phys. Lett.* **96** 142507
[25] Larbalestier D, Gurevich A, Feldmann D M and Polyanskii A 2001 *Nature* **414** 368
[26] Katase T, Ishimaru Y, Tsukamoto A, Hiramatsu H, Kamiya T, Tanabe K and Hosono H 2011 *Nat. Commun.* **2** 409
[27] Hilgenkamp H and Mannhart J 2002 *Rev. Mod. Phys.* **74** 485
[28] Cybart S A, Cho E Y, Wong T J, Wehlin B H, Ma M K, Huynh C and Dynes R C 2015 *Nat. Nanotechnol.* **10** 598
[29] Kasaei L, Melbourne T, Manichev V, Feldman L C, Gustafsson T, Chen K, Xi X X and Davidson B A 2018 *AIP Adv.* **8** 075020
[30] Wang Y T, LeFebvre J C, Cho E Y, McCoy S J, Li H, Gu G D, Kadowaki K and Cybart S A 2021 *IEEE Trans. Appl. Supercond* **31** 1100104
[31] Kano M, Kohama Y, Graf D, Balakirev F, Sefat A S, McGuire M A, Sales B C, Mandrus D and Tozer S W 2009 *J. Phys. Soc. Jpn.* **78** 084719
[32] Kasaei L, Manichev V, Li M, Feldman L C, Gustafsson T, Colantes Y, Hellstrom E, Demir M, Acharya N, Bhattarai P, Chen K, Xi X X and Davidson B A 2019 *Supercond. Sci. Technol.* **32** 095009
[33] Yuan P, Xu Z, Li C, Quan B, Li J, Gu C and Ma Y 2018 *Supercond. Sci. Technol.* **31** 025002
[34] Chen Z W, Li Y L, Zhu R, Xu J, Xu T Q, Yin D L, Cai X W, Wang Y, Lu J M, Zhang Y and Ma P 2022 *Chin. Phys. Lett.* **39** 077402
[35] Muller B, Karrer M, Limberger F, Becker M, Schroppel B, Burkhardt C J, Kleiner R, Goldobin E and Koelle D 2019 *Phys. Rev. Appl.* **11** 044082
[36] Vale L R, Ono R H and Rudman D A 1997 *IEEE Trans. Appl. Supercond.* **7** 3193